Inorg. Chem. **2005**, *44*, 5629–5635

Mössbauer Spectroscopy of Bucky Ferrocenes: Lattice Dynamics and Motional Anisotropy of the Metal Atom

Rolfe H. Herber,*,† Israel Nowik,† Yutaka Matsuo,‡ Motoki Toganoh,§ Yoichiro Kuninobu,§ and Eiichi Nakamura*,‡,§

Racah Institute Of Physics, The Hebrew University of Jerusalem, 91904 Jerusalem, Israel, and Nakamura Functional Carbon Cluster Project, ERATO, Japan Science and Technology Agency, and Department of Chemistry, The University of Tokyo, Hongo, Bunkyo-Ku, Tokyo 113-0033, Japan

Received February 18, 2005

Temperature-dependent ^{57}Fe Mössbauer effect spectroscopy has been used to elucidate the metal atom dynamics in three neutral and two cationic bucky ferrocenes. For the three diamagnetic complexes Fe($C_{60}H_5$)Cp (**1**), Fe($C_{60}Me_5$)Cp (**2**), and Fe($C_{60}Ph_5$)Cp (**3**), the metal atom motion is anisotropic and the temperature dependence of the mean-square amplitude of vibration of the metal atom at a number of temperatures is reported. The Mössbauer lattice temperatures have been determined and compared to the parent ferrocene (**6**). The synthesis and X-ray crystal structure of **3** have been determined at 153(2) K, and the ^{1}H and ^{13}C NMR spectra have been recorded. The cationic complexes derived from **2** and **3** show spin–lattice relaxation. The relaxation rate appears insensitive to the nearest-neighbor environment of the metal atom in this pair.

Introduction

The quest for the design and construction of molecular devices which can function as active components in electronic circuits has received a great deal of attention in recent years. In particular, the incorporation of C_{60} (buckyball) in such structures has been the focus of intense research in this field due to the possibilities of modifying the buckyball structure with chemical ligands which themselves provide possible electron pathways and connections to the larger environment.[1−4] Among such ligands are organometallic moieties which can provide the intermolecular connectivity needed for such devices.

In view of its centrality in the development of modern organometallic chemistry, ferrocene, Fe(η^5-Cp)$_2$ (Cp = C_5H_5), has been the subject of an extremely large array of physicochemical techniques designed to lead to a full understanding of the structure, bonding, thermodynamic, and kinetic properties of this unique molecule, first described[5] by Kealy and Pauson in 1951. Among these techniques was the phenomenon of resonant γ-ray scattering (Mössbauer effect, ME); in fact, ferrocene was the first iron-organometallic compound studied by this spectroscopy,[6] and a large literature has developed in this field.

Of particular interest in this context is the possibility of using temperature-dependent ME spectroscopy to elucidate the detailed motion of the iron atoms in such compounds and relating this to the numerous detailed single-crystal X-ray diffraction studies which have also been reported[7] at a variety of temperatures. The recent discovery of the synthesis of

* Authors to whom correspondence should be addressed. E-mail: herber@vms.huji.ac.il (R.H.H.); nakamura@chem.s.u-tokyo.ac.jp (E.N.).
† The Hebrew University of Jerusalem.
‡ Nakamura Functional Carbon Cluster Project, ERATO, JST.
§ The University of Tokyo.

(1) Porath, D.; Levy, Y.; Tarabiah, M.; Millo, O. *Phys. Rev. B* **1997**, *56B*, 9829−9833.
(2) Zeng, C.; Wang, H.; Wang, B.; Yang, J.; Hou, J. G. *Appl. Phys. Lett.* **2000**, *77*, 395−397.
(3) Gutierrez, R.; Fagas, G.; Cuniberti, G.; Grossmann, F.; Schmidt, R.; Richter, K. *Phys. Rev. B* **2002**, *65*, 34101−34104.
(4) Cunniberti, G.; Gutierrez, R.; Fagas, G.; Grossmann, F.; Richter, K.; Schmidt, R. *Physica* **2002**, *E12*, 749−752.
(5) (a) Kealy, T. J.; Pauson, P. L. *Nature (London)* **1951**, *168*, 1039−1040. See also the special volume devoted to ferrocene: *J. Organomet. Chem.* **2001**, *637−639*, 3−26 and references therein.
(6) Herber, R. H.; Werthewim, G. K. In *Proceedings of the Second International Conference on the Mössbauer Effect*, Saclay, France, 1961; Compton, D. M. J., Schoen, A. H., Eds.; J. Wiley and Sons: New York, 1962. See also: Zahn, U., Kienle, P.; Eicher, H. In *Proceedings of the Second International Conference on the Mössbauer Effect*, Saclay, France, 1961; Compton, D. M. J., Schoen, A. H., Eds.; J. Wiley and Sons: New York, 1962.
(7) Brock, C. P.; Fu, Y. *Acta Crystallogr. B* **1997**, *53*, 928−938 and references therein.

10.1021/ic050251e CCC: $30.25
Published on Web 07/07/2005

Chart 1

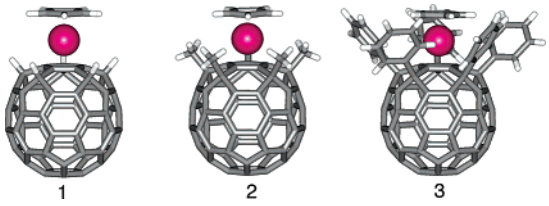

bucky ferrocenes,[8,9] in which the local bonding environment around the iron atom is similar to that in ferrocene itself, but in which the more distant environment can take on a variety of architectures, has made it desirable to study the details of the lattice dynamics and motional anisotropy of the iron atom in these ferrocenoids. For instance, it is expected that motion of the iron atom of a bulky bucky ferrocene (i.e. pentaaryl bucky ferrocene **3**) is much smaller than that of a less bulky one (i.e. pentahydro bucky ferrocene **1**) (Chart 1). This study was conceived to elucidate these properties of the metal atom in both neutral and one-electron oxidation products of a number of bucky ferrocenes and to relate this to the molecular level architecture of these compounds. Among the compounds for which ME parameters are discussed in detail in the present discussion are $Fe(C_{60}H_5)Cp$ (**1**), $Fe(C_{60}Me_5)Cp$ (**2**), $Fe(C_{60}Ph_5)Cp$ (**3**), $[Fe(C_{60}Me_5)Cp]^+[SbCl_6]^-$ (**4**), and $[Fe(C_{60}Ph_5)Cp]^+[SbCl_6]^-$ (**5**) as well as comparison data for ferrocene (**6**).

Experimental Section

General Procedure for the Synthesis of Bucky Ferrocenes. Syntheses and manipulation of materials were carried out under nitrogen or argon atmosphere using standard Schlenk techniques. THF was distilled from Na/K alloy and thoroughly degassed by trap-to-trap distillation. Benzonitrile was distilled from CaH_2. $C_{60}Ph_5H$,[10] $C_{60}Me_5H$,[11] $Fe(\eta^5\text{-}C_{60}H_5)(\eta^5\text{-Cp})$ (**1**),[8] and $Fe(\eta^5\text{-}C_{60}Me_5)(\eta^5\text{-Cp})$ (**2**)[9] were prepared according to the literature. $[FeCp(CO)_2]_2$ and $[(4\text{-}BrC_6H_4)_3N][SbCl_6]$ were purchased from Acros Organics and Aldrich and used as received. ^1H (400 MHz) and ^{13}C (100 MHz) NMR spectra were recorded using a JEOL EX-400 spectrometer. Proton chemical shift are reported relative to Me_4Si ($CDCl_3$) at δ 0.00 ppm or residual solvent peaks ($CDCl_3$ at δ 7.26 ppm; THF-d_8 at δ 1.73 and 3.58 ppm). Carbon chemical shift values are reported relative to $CDCl_3$ at δ 77.00 ppm or THF-d_8 at δ 25.20 and 67.40 ppm. Other spectra were recorded on the following instruments: IR, JASCO IR-420 and ReactIR 1000; UV/vis spectra, HITACHI U3500 and Shimadzu SPD-6A; mass spectra, Shimadzu LCMS-QP8000 and JEOL Accu TOF (JMS-T100LC).

Synthesis of $Fe(\eta^5\text{-}C_{60}Ph_5)(\eta^5\text{-Cp})$ (3). A mixture of $C_{60}Ph_5H$ (200 mg, 0.181 mmol) and $[FeCp(CO)_2]_2$ (320 mg, 0.900 mmol) in benzonitrile (40.0 mL) was stirred at 180 °C for 20 h. After evaporation of the solvent, the crude mixture was diluted with toluene, and the solution was passed through a pad of silica gel. Solvent was removed in vacuo, and the mixture was recrystallized from CS_2/hexane to obtain the title compound as air-stable dark red microcrystals (171 mg, 77% yield): ^1H NMR (400 MHz, $CDCl_3$) δ 3.21 (s, 5H, Cp), 7.33−7.37 (m, 10H, Ph), 7.39−7.40 (m. 5H, Ph), 7.93−7.95 (m, 10H, Ph); ^{13}C NMR (100 MHz, $CDCl_3$/CS_2 = 1/1) δ 58.23 (5C), 73.20 (5C), 92.47 (s, 5C), 127.41 (5C), 127.47 (10C), 128.97 (10C), 142.82 (5C), 142.92 (10C), 143.66 (10C), 147.03 (5C), 147.81 (10C), 148.06 (5C), 152.14 (10C); IR (CS_2) $\nu_{C-H\ (Cp)}/cm^{-1}$ 3101; UV−vis (1.0×10^{-5} mol·L^{-1} in CH_2Cl_2) λ_{max} (ϵ) 260 (84 700), 295 (57 300, shoulder), 351 (23 600), 394 (12 200), 475 (4330, shoulder) nm; HRMS (APCI+) calcd for $C_{95}H_{30}Fe$ (M^+) 1226.1697, found 1226.1695.

Preparation of Fe(III) Complexes. To a solution of **2** (151 mg, 0.164 mmol) in THF (300 mL) was added $[(4\text{-}BrC_6H_4)_3N][SbCl_6]$ (147 mg, 0.181 mmol). After the solution was stirred at 25 °C for 5 h, the solvent was removed in vacuo. The solid was washed several times with H_2O, EtOH, and $CHCl_3$. After the solid was dried in vacuo, $[Fe(\eta^5\text{-}C_{60}Me_5)(\eta^5\text{-Cp})][SbCl_6]$ (**4**) (170 mg, 83%) was obtained as a reddish brown solid. Characterization of **4** was obtained by means of an ESR measurement, showing *g*-values of 3.94 ($g_{\parallel}$) and 1.57 ($g_{\perp}$) at 4.4 K. Similarly, oxidation of **3** (99.2 mg, 0.0808 mmol) with $[(4\text{-}BrC_6H_4)_3N][SbCl_6]$ (72.6 mg, 0.0889 mmol) in THF (70.0 mL) gave $[Fe(\eta^5\text{-}C_{60}Ph_5)(\eta^5\text{-Cp})][SbCl_6]$ (**5**) (62.2 mg, 49%) as a reddish brown solid. Samples of these cationic complexes **4** and **5** contain starting materials **2** and **3**, respectively, as minor components as judged by Mössbauer spectroscopic analyses.

Mössbauer Spectroscopy. The details of temperature-dependent ME spectroscopy, making use of the 14.4 keV radiation of ^{57}Fe, have been discussed earlier.[12] Spectrometer calibration was effected using a ~50 mCi ^{57}Co source (Rh matrix) in conjunction with an α-Fe absorber at room temperature, and all isomer shifts reported herein are with reference to the centroid of such spectra. Temperature control was effected using a high-gain feedback controller together with a Cu−Constantan thermocouple, and the temperatures reported are judged to be stable to ±0.2 deg over the time intervals (5−24 h) required to accumulate the ME data at a given temperature. Powdered samples of the air-stable compounds were transferred to plastic sample holders and subjected to spectroscopic examination without further treatment.

X-ray Crystallographic Analysis. Single crystals of **3** were obtained by recrystallization by slow diffusion of ethanol into a CS_2 solution of **3**. The X-ray data sets were collected at 153 and 293 K on a MacScience DIP2030 imaging plate diffractometer equipped with graphite-monochromated Mo Kα radiation (λ = 0.710 69). Crystal data and data statistics for **3** are summarized in Table 3. The structure of **3** was solved by the direct methods, SIR-97.[13] The positional parameters and thermal parameters of non-hydrogen atoms were refined anisotropically on F^2 by the full-matrix least-squares method, using SHELXL-97.[14] All non-hydrogen atoms of **3** were anisotropically refined. Hydrogen atoms

(8) Toganoh, M.; Matsuo, Y.; Nakamura, E. *J. Am. Chem. Soc.* **2003**, *125*, 13974−13975.
(9) (a) Sawamura, M.; Kuninobu, Y.; Toganoh, M.; Matsuo, Y.; Yamanaka, M.; Nakamura, E. *J. Am. Chem. Soc.* **2002**, *124*, 9354−9355. (b) Nakamura, E. *Pure Appl. Chem.* **2003**, *75*, 427−434. (c) Matsuo, Y.; Nakamura, E. *Organometallics* **2003**, *22*, 2554−2563. (d) Matsuo, Y.; Kuninobu, Y.; Ito, S.; Nakamura, E. *Chem. Lett.* **2004**, *33*, 68−69.
(10) (a) Sawamura, M.; Iikura, H.; Nakamura, E. *J. Am. Chem. Soc.* **1996**, *118*, 12850−12851. (b) Iikura, H.; Mori, S.; Sawamura, M.; Nakamura, E. *J. Org. Chem.* **1997**, *62*, 7912−7913. (c) Sawamura, M.; Iikura, H.; Ohama, T.; Hackler, U. E.; Nakamura, E. *J. Organomet. Chem.* **2000**, *599*, 32−36.
(11) (a) Sawamura, M.; Toganoh, M.; Kuninobu, Y.; Kato, S.; Nakamura, E. *Chem. Lett.* **2000**, 270−271. (b) Nakamura, E.; Sawamura, M. *Pure Appl. Chem.* **2001**, *73*, 355−359.
(12) (a) Herber, R. H.; Nowik, I. *Hyperfine Interact.* **2001**, *136/137*, 699−703. (b) Herber, R. H.; Nowik I. *Solid State Sci.* **2002**, *4*, 691−694.
(13) Altomare, A.; Burla, M. C.; Camalli, M.; Cascarano, G. L.; Giacovazzo, C.; Guagliardi, A.; Moliterni, A. G. G.; Polidori, G.; Spagna, R. *J. Appl. Crystallogr.* **1999**, *32*, 115−119.
(14) Sheldrick, G. M. *Program for the Solution of Crystal Structures*; University of Göttingen: Göttingen, Germany, 1997.

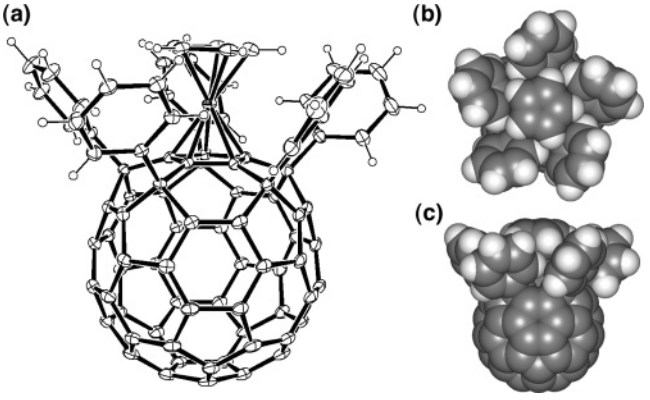

Figure 1. Crystal structure of **3**: (a) ORTEP drawing with 30% probability level; (b) top view of a CPK model; (c) side view of a CPK model of **3** ellipsoids. In (a), the solvent molecule (CS_2) in the unit cell is omitted for clarity.

were placed at calculated positions and refined "riding" on their corresponding carbon atoms. In the subsequent refinement, the function $\Sigma\omega(F_o^2 - F_c^2)^2$ was minimized, where $|F_o|$ and $|F_c|$ are the observed and calculated structure factor amplitudes, respectively. The agreement indices are defined as $R1 = \Sigma(||F_o| - |F_c||)/\Sigma|F_o|$ and $wR2 = [\Sigma\omega(F_o^2 - F_c^2)^2/\Sigma(\omega F_o^4)]^{1/2}$. Data have been deposited with the Cambridge Crystallographic Data Centre as supplementary publication no. CCDC-271687.

Results and Discussion

Synthesis and X-ray Structure Analysis of Bucky Ferrocenes. We communicated earlier the synthesis and characterizations of pentahydro bucky ferrocene, Fe($C_{60}H_5$)Cp (**1**),[8] and pentamethyl bucky ferrocene, Fe($C_{60}Me_5$)Cp (**2**).[9] Pentaphenyl bucky ferrocene Fe($C_{60}Ph_5$)Cp (**3**) was obtained in a manner similar to the synthesis of **2** (eq 1). Heating $C_{60}Ph_5H$ and $[FeCp(CO)_2]_2$ in benzonitrile at 180 °C for 20 h directly afforded **3**, which was obtained as air- and moisture-stable dark red crystals in 77% isolated yield after purification by silica gel column chromatography and recrystallization from a mixture of CS_2 and ethanol. The structure of **3** was determined by ^1H and ^{13}C NMR and high-resolution APCI-TOF-MS as well as single-crystal X-ray diffraction study. The ^1H and ^{13}C NMR spectra of bucky ferrocene **3** exhibited C_{5v} symmetric signal patterns for the $C_{60}Ph_5$ and Cp ligands. This result suggests that the $C_{60}Ph_5$ and Cp ligands rotate rapidly in solution.

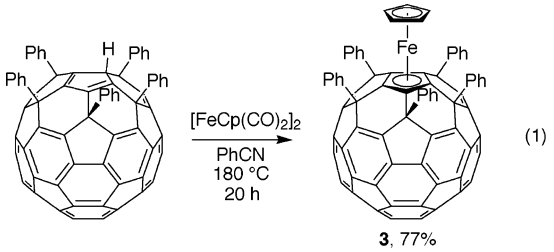

Figure 1 shows the crystal structure of **3**. Whereas the averaged bond lengths Fe−C($C_{60}Ph_5$) (2.084 Å) of **3** are quite similar to those of **2** (2.087 Å),[9a] the bond lengths Fe−C(Cp) (2.062 Å) are much longer than those of **2** (2.033 Å). This is probably because of the steric hindrance between the Cp ligand and the five phenyl groups of the $C_{60}Ph_5$ ligand which can be seen in the 3D structure of **3** (Figure 1b,c).

Cationic bucky ferrocenes, [Fe(η^5-$C_{60}Me_5$)(η^5-Cp)][$SbCl_6$] (**4**) and [Fe(η^5-$C_{60}Ph_5$)(η^5-Cp)][$SbCl_6$] (**5**), were obtained by oxidation of **2** and **3** with an aminium salt, [(4-$BrC_6H_4)_3N$]-[$SbCl_6$] (eq 2). As the oxidant was added to a THF solution of **2** or **3**, the color of the solution changed from light orange to dark orange, while the dark blue color of the aminium salt disappeared immediately. Compounds **4** and **5** are soluble to some extent in benzonitrile but are insoluble in common solvents (i.e, chloroform, THF, toluene, hexane, methanol, ethanol, acetonitrile, and carbon disulfide). Compounds **4** and **5** are ESR active. At 4.4 K, *g*-values for **4** are 3.94 ($g_{||}$) and 1.57 ($g_{\perp}$), which are comparable to those of ordinary ferrocenium cations such as $FeCp_2^+$.[15]

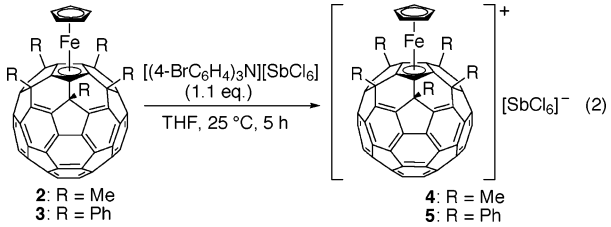

Mössbauer Studies. The ME spectra of neutral ferrocenoids, incorporating a single metal atom/molecule, consist of a well-resolved doublet which can be analyzed in terms of its isomer shift (IS), quadrupole splitting (QS), area under the resonance curve (*A*), the doublet asymmetry ratio (*R*), and parameters derived therefrom and are summarized in Table 1.

Compound 1. A typical spectrum of **1** at 90 K is shown in Figure 2. The total number of counts/channel in this spectrum is $\sim 1.3 \times 10^6$, and it is clear that this is an optically "thin" absorber. The ME hyperfine parameters at 90 K for **1** are summarized in Table 1 which also lists the corresponding values for the parent ferrocene (**6**) for comparison. It will be seen that both the IS(90 K) and QS(90 K) values are very similar for the two solids. Both the temperature dependencies of the IS and ln(*A*) parameters suggest a slightly "harder" bonding environment for the iron atom in the bucky ferrocene than in the parent solid, but the difference is small. It is noteworthy that the temperature dependence of the mean-square amplitude of vibration (msav), proportional to ln *A*(*T*), for **1** is well fitted by a linear regression, with a slope of $-(6.50 \pm 0.22) \times 10^{-3}$ K^{-1}, $R = 0.986$ for 14 data points, in contrast to the corresponding data for ferrocene which shows two crystallographic phase transitions at ~170 and ~250 K, as noted earlier.[16]

It is, of course, evident from Figure 2 that the area ratio, *R*, defined as the ratio of the spectral area at velocities more positive than the spectrum centroid, *A*(+), to that at more negative velocities, *A*(−), is significantly different from unity. There are two principal reasons for this phenomenon: texture

(15) Prins, R.; Reinders, F. J. *J. Am. Chem. Soc.* **1969**, *91*, 4929−4931.
(16) (a) Naruse, M.; Sorai, M.; Sakiyama, M. *Mol. Cryst. Liq. Cryst.* **1983**, *101*, 219−234. (b) Edwards, J. W.; Kington, G. L.; Mason, R. *Trans. Faraday Soc.* **1960**, *56*, 660−667. (c) Ogasahara, K.; Sorai, M.; Suga, H. *Chem. Phys. Lett.* **1979**, *68*, 457−460.

Table 1. Mössbauer Parameters of the Compounds Discussed in the Text[a]

	1	2	3	4	5	6	units
IS(90)	0.547(5)	0.575(4)	0.586(4)	0.537(3)	0.612(3)	0.537(1)	mm/s
QS(90)	2.401(5)	2.475(4)	2.471(4)	0.185(3)	0.108(3)	2.418(1)	mm/s
$-$d(IS)/dT	4.73(14)[b]	5.36(5)[d]	5.55(5)[f]	curv	4.97(24)	5.12(6)	$\times 10^{-4}$ mm/s K
$-$d ln A/dT	6.50(22)[c]	7.42(17)[e]	4.71(5)[g]	$\sim$7.2(2)[b]	$\sim$7.0(5)[c]	8.78(14)	$\times 10^{-3}$/K
M_{eff}	87(3)	78(2)	75(1)	94 ± 10[d]	84 ± 4[e]	81(2)	Da
Θ_{M}	116	116	148			104	K

[a] The parenthetical numbers are the errors in the last place(s) of the reported value. [b] T range = 170−320 K. [c] T range = 90−320 K. [d] T range = 210−370 K. [e] T range = 210−370 K. [f] T range = 210−375 K. [g] T range = 90−375 K.

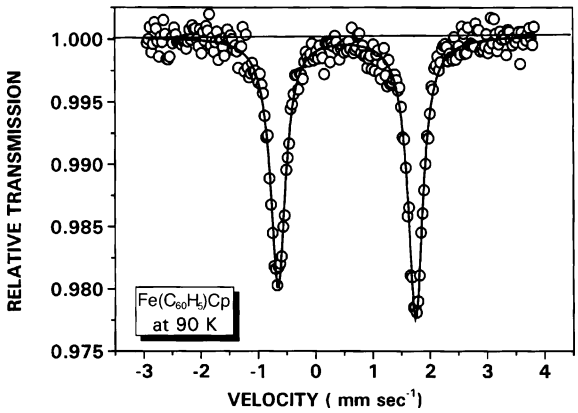

Figure 2. ^{57}Fe Mössbauer spectrum of **1** at 90 K. The zero point of the velocity scale is the centroid of a room-temperature α-Fe calibration absorber spectrum.

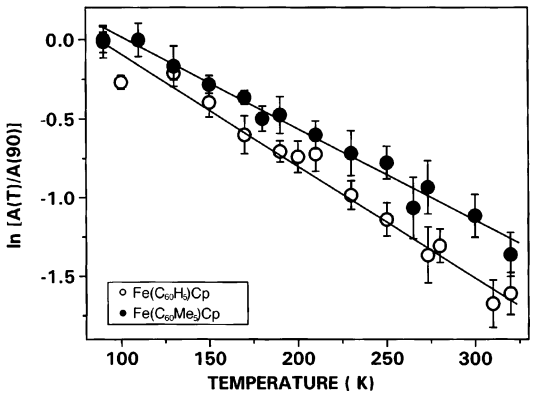

Figure 3. Temperature dependence of the recoil-free fraction for **1** (open points) and **2** (filled points) normalized to the 90 K data.

and vibrational anisotropy. It is readily possible to distinguish between these two effects, since the former is essentially temperature independent, whereas the latter evidences a clear change with T, as is the case with the presently discussed complexes. Moreover, this T dependence can be quantitatively related to the motional anisotropy of the iron atom with respect to the (local) molecular symmetry axis, the so-called Gol'danskii−Karyagin effect (GKE), and thus to the difference in the vibrational amplitudes in the two directions, that is, parallel and perpendicular to the local C_5 axis through the metal atom. This vibrational anisotropy has been reported[17] in a number of other ferrocene related solids and appears to be a general phenomenon in these organometallics as will be discussed more fully below for **2** and **3**. In this context it is obviously clear that the "texture" and GKE effects are not mutually exclusive. To estimate the contribution of the former, a ME spectrum of **1** was acquired at 4.2 K, a temperature at which the GKE is assumed to be negligible. In this spectrum, R was found to be 1.049 ± 0.005, and this 5% contribution to R due to texture has been corrected for in the vibrational amplitude calculations to be discussed below.

In a separate ME experiment at room temperature, using the magnetic field effect discussed in detail by Collins,[18] it was determined that the quadrupole interaction in these compounds is positive, and hence, the measured $R > 1$ means that the motion parallel to the (local) molecular symmetry axis, $\langle (x^2)_{\mathrm{para}} \rangle$, is smaller than the corresponding vibrational amplitude perpendicular to this axis, $\langle (x^2)_{\mathrm{perp}} \rangle$ as is true of ferrocene itself. The assumptions underlying the relationship between the temperature dependence and the recoil-free fraction have been discussed previously.[19] A further simplifying assumption made in this analysis is that $T > \Theta_{\mathrm{M}}/2$, where Θ_{M} is the Mössbauer lattice temperature,[20] so that the temperature dependence of f scales directly with the area under the resonance curve. Since $f = \exp(-k^2\langle x^2 \rangle)$, where k is the wavenumber of the 14.4 keV γ ray of ^{57}Fe, these data permit the calculation of $\langle x^2_{\mathrm{ave}} \rangle$ for the iron atom. The temperature dependence of the recoil-free fraction, f, for **1** is shown graphically in Figure 3, and the significance of these results will be discussed in further detail below. Further, from the temperature dependence of the area ratio, R, and making the assumption that $\langle x^2_{\mathrm{ave}} \rangle = 1/3\langle x^2_{\mathrm{para}} \rangle + 2/3\langle x^2_{\mathrm{perp}} \rangle$, it is possible to calculate the difference in vibrational amplitude parallel and perpendicular to the (local) molecular (C_5) symmetry axis. The results of these calculations for **1** are summarized graphically in Figure 4 in which the temperature dependence of $k^2\langle x^2_{\mathrm{par}} \rangle$ (▲) and $k^2\langle x^2_{\mathrm{perp}} \rangle$ (▼) are compared to the values calculated for $\Theta_{\mathrm{M}} = 116$ K and $M_{\mathrm{eff}} = 87$ Da, as indicated by the solid line.

Compound 2. The ME hyperfine parameters and data derived therefrom are included in the summary of Table 1. It is clear that both the IS and QS parameters at 90 K are little different from those of compound **1** and the substitution of methyl groups for hydrogen in the five-membered ring ligated to the metal atom has little effect on the electronic environment around Fe. This is in consonance with earlier data which showed that ring substitution does not appreciably

(17) The interested reader is referred to the following: *J. Organomet. Chem.* **2001**, *637*−*639*. This includes numerous X-ray crystal structure data which reflect this iron atom motional anisotropy.
(18) Collins, R. L. *J. Chem. Phys.* **1965**, *42*, 1072−1080.
(19) Nowik, I.; Herber, R. H. *J. Phys. Chem. Solids* **2003**, *64*, 313−317.
(20) Herber, R. H. In *Chemical Mössbauer Spectroscopy*; Herber, R. H. Ed.; Plenum Press: New York, 1984; Chapter VII.

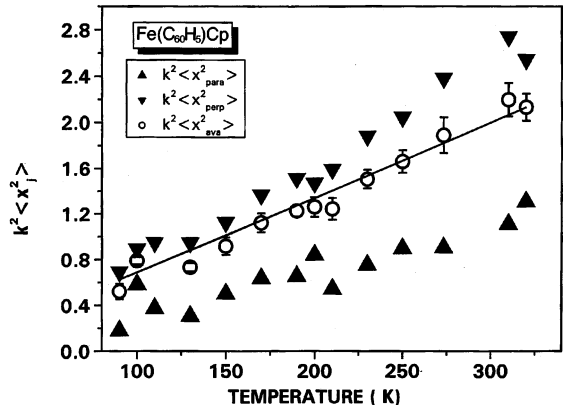

Figure 4. Temperature dependence of $k^2\langle x^2\rangle$ for **1**. The solid line reflects the calculation for $M_{\text{eff}} = 89$ Da and $\Theta_M = 116$ K as discussed in the text.

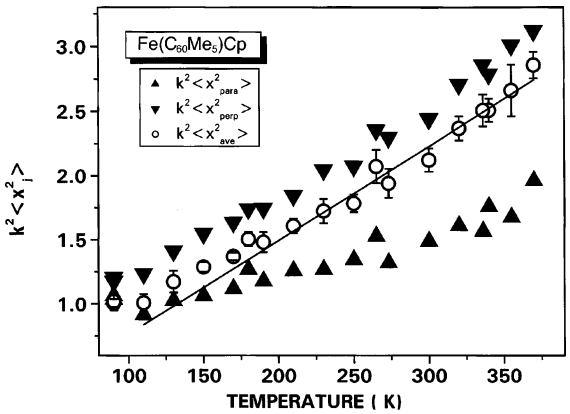

Figure 5. Temperature dependence of $k^2\langle x^2\rangle$ for **2**. The solid line reflects the calculation for $M_{\text{eff}} = 78$ Da and $\Theta_M = 116$ K as discussed in the text.

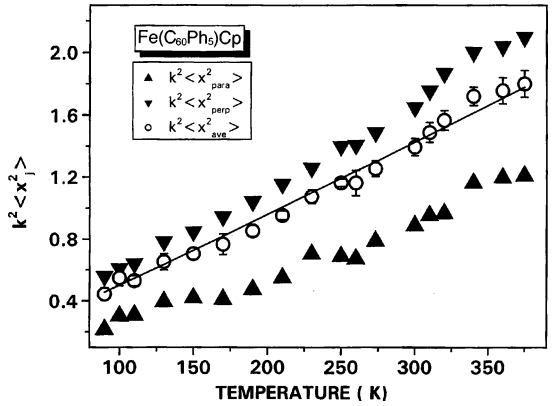

Figure 6. Temperature dependence of $k^2\langle x^2\rangle$ for **3.** The solid line reflects the calculation for $M_{\text{eff}} = 75$ Da and $\Theta_M = 148$ K as discussed in the text.

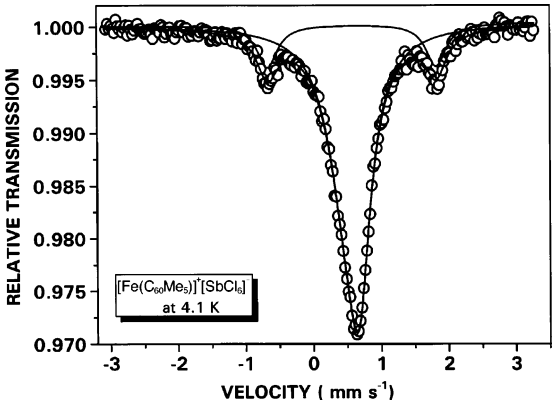

Figure 7. ^{57}Fe Mössbauer spectrum of **4** at 4.1 K. The doublet absorbance is ascribed to the presence of a small quantity of the neutral parent compound (**2**) used to prepare **4**.

affect the ring bonding to the metal atom. The temperature dependence of the IS and the recoil-free fraction are slightly different in **2** as compared to **1**, leading to a slightly smaller M_{eff}[20] but having the same Θ_M. As in the case of **1**, above, a 4.2 K ME spectrum yielded an R value of 1.05 ± 0.01, and again this "texture" contribution was corrected for in the subsequent data analysis. Using the linear approximation discussed above, it is again possible to extract the temperature dependence of f for the metal atom in this compound, and the results are again included in Figure 3 and in Table 1. As in the case of **1**, R is a temperature-dependent parameter and can be used to extract $\langle x_{\text{perp}}{}^2\rangle$ and $\langle x_{\text{para}}{}^2\rangle$ from the data; see below. In this context it should be noted that the $U_{i,j}$ values extracted from single-crystal X-ray diffraction data for **2** are in the ratio of 1:1.05:1.16 at 293 K and 1:1.25:1.76 at 153 K. The $\langle x^2_j\rangle$ values are summarized graphically in Figure 5 using the same conventions as given for Figure 4. The solid line in this figure corresponds to $k^2\langle x^2_{\text{ave}}\rangle$ calculated for $M_{\text{eff}} = 78$ Da and $\Theta_M = 116$ K.

Compound 3. In the case of the pentaphenyl bucky ferrocene, the ME data showed evidence for the presence of a small impurity in the spectra, with an IS(90) and QS(90) of 0.282(9) and 0.369(7) mm s^{-1}, respectively. The fractional area due to this impurity was found to be ~5% at 90 K but larger at the higher temperatures and has been corrected for in the calculation of the recoil-free fraction data. Except for the observation that this impurity has a higher Θ_M than the major constituent, no further attempt was made to identify its nature more exactly. As before, the ME hyperfine parameters are summarized in Table 1 and with the exception of the temperature dependence of the recoil-free fraction are similar to those listed for **1** and **2**. For **3**, the vibrational anisotropy is reflected in the ratio of the $U_{i,j}$ values which correspond to 1:1.03:1.23 at 293 K and 1:1.13:1.46 at 153 K. Of interest with respect to the pentaphenyl compound is the temperature dependence of f, which is significantly smaller than what was observed for the $C_{60}H_5$ and $C_{60}Me_5$ compounds, as will be discussed below. As before, calculation of the parallel and perpendicular values for $k^2\langle x^2_j\rangle$ are summarized graphically in Figure 6, again using the same convention as in Figure 4. The solid line corresponds to $k^2\langle x^2_{\text{ave}}\rangle$ calculated for $M_{\text{eff}} = 75$ Da and $\Theta_M = 148$ K.

From the data summarized in Figures 4−6, it is immediately seen that while there is relatively little difference in $k^2\langle x^2_j\rangle$ for the $C_{60}H_5$ and $C_{60}Me_5$ compounds, a significant decrease in this parameter at all temperatures is noted for the $C_{60}Ph_5$ homologue.

Compound 4. A typical ME spectrum of the one-electron oxidation product of **2** at 90 K is shown graphically in Figure 7 in which the major resonance reflects the nearly complete collapse of the QS interaction in this cation, as has been reported[21] for numerous other ferrocenium-related complexes, in consonance with the pioneering study of Collins.[18] While the IS(90) is nearly the same as it is for the parent **2**, the

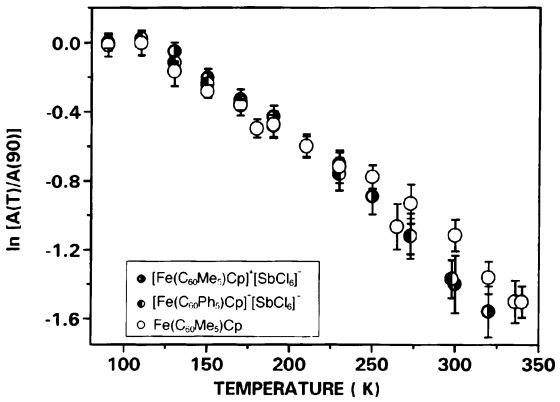

Figure 8. Temperature dependence of the recoil-free fraction for **2**, **4**, and **5**. While there is some curvature noted in these experimental points at low temperatures, only the high-temperature-limiting slopes were used to calculate M_{eff} and Θ_{M} from these data.

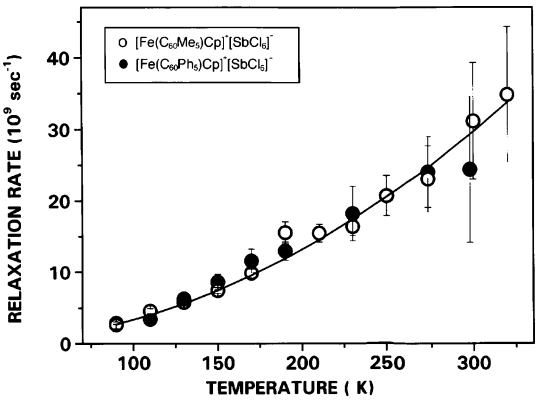

Figure 9. Temperature dependence of the spin−lattice relaxation rates of the iron atom in **4** (open points) and **5** (closed points). The two data sets are normalized to the 90 K values to afford intersample comparison as discussed in the text.

QS(90) value has decreased from 2.48 to 0.19 mm s^{-1} on the removal of one electron. It is also noted from Figure 7 that there is evidence for a small but nonnegligible second iron site, especially at the lower temperatures. The hyperfine parameters for this minor component at 90 K are 0.582(3) and 2.486(3) mm s^{-1} for the IS and QS, respectively. The similarity between these values and those reported (Table 1) for pure **2** leave little doubt that this minor component is unoxidized starting material **2** in the sample. The fractional area due to this compound is ∼18% at 4.2 K and falls to ∼8.5% at 300 K, and corrections for the presence of this material have been made in the data reduction where applicable.

The temperature dependence of f for **5** is summarized graphically in Figure 8, which also includes the corresponding data for **6** and **2**. From this figure it is seen that the iron atom in the cationic complex is embedded in a slightly "softer" lattice than is true for the corresponding neutral diamagnetic **2**, although the difference is quite small, an effect which has been previously noted for other ferrocene complexes and their one electron oxidation products. Clearly the presence of the large $SbCl_6^-$ anion in the lattice plays only a very small role in the vibrational characteristics of the iron atom in these structures.

ME spectra of ferrocenium salts can be analyzed in terms of the spin−lattice relaxation rate as has been previously reported from this laboratory.[19] The assumptions inherent in these data treatment have been reviewed earlier, and it is clear that the absolute values of the relaxation rates depend on the values assigned to the magnetic hyperfine field at the metal center. In the absence of detailed information concerning H_{i}, a value of 500 kOe has been arbitrarily assigned to this parameter, so that only comparative values between related compounds have any significance in the present discussion. The temperature dependences of the spin−lattice relaxation rates for **4** and **5** are summarized graphically in Figure 9 in which the 90 K τ datum for **5** (3.83×10^{-9} sec) has been normalized to the 90 K value for **4** (3.52×10^{-9} s), and this ratio (1.09) has been applied over the total T range. Over the indicated temperature range, the two relaxation rates are quite comparable, and clearly the substitution of a phenyl for a methyl group on the five-membered ring ligated to the metal atom does not play a significant role in the spin−lattice relaxation rate of these complexes.

Compound 5. As was true for the ME spectra of **4**, those of **5** evidence the presence of a small starting material **3** with an IS and QS at 90 K of 0.583 ± 0.008 and 2.458 ± 0.008 mm s^{-1}, respectively. The similarity between these values and those observed for the neutral parent, **3**, leave little doubt that this second resonance is due to unoxidized parent compound which has survived the purification process described above. In the subsequent data analysis, the presence of this second site has been taken into consideration.

The temperature dependence of the IS for **4** over the temperature range $90 < T < 320$ K shows some curvature while the corresponding data for **5** are fit by a linear function over the temperature interval $90 < T < 298$ K, but the differences in the two data sets are quite small. The value of M_{eff} calculated for **5** is 84 ± 4 Da, while that for **4** taken over the total temperature range (ignoring the curvature in the data) is 94 ± 10 Da. Clearly the replacement of the five methyl groups in **4** by five phenyl groups in **5** plays a negligible role in the effective vibrating mass of the metal atom in these compounds in agreement with earlier data related to ring substitutions in ferrocenoids.[22]

As noted above, the temperature dependence of the recoil-free fraction for **5** is shown in Figure 8. Although there is some slight curvature in both data sets, it is evident that the data for the two compounds **4** and **5** are quite similar. Moreover, $-\text{d}\ \ln[A(T)/A(90)]/\text{d}\ T$ for **2** and **4** are quite similar, but this similarity does not obtain for the **3**, **5** pair. The relative spin−lattice relaxation rate for **5** as a function of temperature is included in Figure 9.

Significance of the Rmsav Data. As noted above, the recoil-free fraction of the metal atom in these compounds is given by $f = \exp(-k^2\langle x^2\rangle)$. The comparison of values for

(21) (a) Nowik, I.; Herber, R. H. *Inorg. Chim. Acta* **2000**, *310*, 191−195. (b) Herber, R. H.; Hanusa, T. P. *Hyperfine Interact.* **1997**, *108*, 563−575.

(22) Herber, R. H.; Bildstein, B.; Denifl, P.; Schottenberger, H. *Inorg. Chem.* **1997**, *36*, 3586−3594 and references therein.

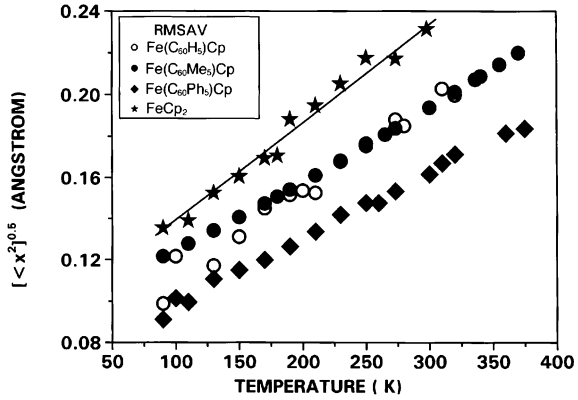

Figure 10. Root-mean-square amplitudes of vibration (rmsav) for the iron atom for the four neutral compounds examined in this study. The linear segment reflects the calculated data for ferrocene with $M_{\text{eff}} = 81$ Da and $\Theta_M = 104$ K.

Table 2. Root-Mean-Square Amplitudes of Vibration (Rmsav) in Å of the Iron Atom at Selected Temperatures for the Compounds Discussed in the Text[a]

temp (K)	**1**	**2**	**3**	**6**
90	0.099	0.097	0.091	0.122
150	0.131	0.121	0.115	0.157
200	0.151	0.139	0.130	0.181
250	0.176	0.154	0.148	0.203
320	0.200	0.181	0.171	0.230

[a] The experimental errors are estimated at ~±4%.

the compounds discussed above is summarized graphically in terms of the rmsav in Å for **1**−**3** in Figure 10 together with the corresponding data for the parent ferrocene, **6** for which the calculated data for $M_{\text{eff}} = 81$ Da and $\Theta_M = 104$ K is indicated by the solid line. It is immediately noted that not only are the values of $k^2\langle x^2\rangle$ smaller at all temperatures for the bucky ferrocenes, as compared to **6**, but the values decrease at a given temperature as the formula weight of the ring substituents (H, Me, and Ph) increases. The inference to be drawn from these regularities is that both the presence of the bulky C_{60} group itself and the molecular weight and/or steric requirements of the ring substituents influence the mean square vibrational amplitude of the metal atom. Moreover, these data permit the calculation of the rmsav of the metal atom as a function of temperature for these compounds, and representative values are given in Table 2.

It should be noted, however, that while the Fe−C(Cp) bond lengths in **3** are significantly larger than those in **2**, as detailed above (X-ray structure), the rmsav of the metal atom in **3** is smaller than that in **2** at all temperatures employed in this study; see Figure 10. The a priori expectation is that the longer Fe−C(Cp) bond lengths in **3** (compared to **2**) would result in a larger $k^2\langle x^2\rangle$ in the former, but this is not what is observed. The origin of this unexpected difference is not apparent from the presently available experimental data.

Table 3. Crystal Data and Structure Analysis Results for **3**·CS_2

formula	$C_{96}H_{30}FeS_2$
cryst system	orthorhombic
space group	$P2_12_12_1$ (No. 19)
a, Å	15.188(5)
b, Å	17.395(5)
c, Å	20.561(5)
α, deg	90
β, deg	90
γ, deg	90
V, Å^3	5432(1)
Z	4
T, K	153(2)
cryst size, mm	0.52, 0.18, 0.12
$2\theta_{\text{min}}$, $2\theta_{\text{max}}$, deg	4.6, 51.18
no. reflcns measd (unique)	9394
no. reflcns measd ($I > 2\sigma(I)$)	8207
no. params	893
R, R_w ($I > 2\sigma(I)$)	0.0536, 0.0619
R1, wR2 (all data)	0.1373, 0.1445
GOF on F^2	1.03

Summary and Conclusions

The synthesis and crystal structure of Fe($C_{60}Ph_5$)Cp is reported together with ^{1}H and ^{13}C NMR and IR data. This compound, together with its $C_{60}H_5$ and $C_{60}Me_5$ homologues, has been examined by temperature-dependent ^{57}Fe Mössbauer spectroscopy in an effort to elucidate the dynamics and anisotropy of the metal atom motion. The vibrational amplitude of the iron atom of **3** was found to be clearly smaller than that of **1**. In addition, two cationic complexes ($SbCl_6^-$ salts) derived from the $C_{60}Me_5$ and $C_{60}Ph_5$ neutral precursors have been similarly characterized. In the case of the neutral complexes, the observation of a temperature-dependent area ratio parameter (Gol'danskii−Karyagin effect) has made it possible to extract root-mean-square vibrational amplitudes of vibration of the metal atom parallel and perpendicular to the local C_5 axis. The two cationic complexes (**4** and **5**) relax primarily by a spin−lattice mechanism which appears to be insensitive to the detailed local molecular architecture around the Fe atom.

Acknowledgment. This research was supported by a Grant-in-Aid for Scientific Research (Specially Promoted Research) and the 21st Century COE programs for Frontiers in Fundamental Chemistry from Monbukagaku-sho, Japan. We thank Frontier Carbon Corp. for a generous supply of [60]fullerene.

Supporting Information Available: CIF file including lists of positional parameters, thermal displacement parameters, bond lengths, and bond angles for **3**. This material is available free of charge via the Internet at http://pubs.acs.org.

IC050251E